

UNIVERSITY OF NEBRASKA-LINCOLN
2017-2018 MIDWEST HIGH POWER ROCKETRY COMPETITION

Husker Rocketry Flight Readiness Report

Team Leads:

Dillon Margritz, dillondmargritz@gmail.com, (308) 325-8466
Conner Vokoun, vokounc@gmail.com, (402) 419-3921
Brandon Warren, bwarren109@gmail.com, (402) 525-3707

Team Members:

Quinn Brandt, Joseph Broadway, Eric Burbach, Nathan Jensen, Grant King, Bricen Margritz, Nathan Mann, Elizabeth Spaulding, Cameron Svoboda, Kenneth Thomason, Stephanie Vavra, and Emily Welchans

Team Faculty Adviser:

Karen Stelling, kstelling2@unl.edu, (402) 472-5253
Department of Mechanical and Materials Engineering, UNL

Team Mentor:

Thomas Kernes, tkernes@buckwestern.com

Submitted: May 9th, 2018

Contents

1 Recap of Rocket Design	4
1.1 Fuselage Specifics and Dimensioning	4
1.2 Internal Components of Booster Section	5
1.3 Diagram of Rocket	5
1.4 Construction Techniques	5
1.5 Stability Analysis	7
1.6 AV-Bay Design	8
1.6.1 Hardware	8
1.6.2 Flight Avionics	9
1.7 Constructed For Safe Flight and Landing	10
1.7.1 Structural Analysis	10
1.7.2 Recovery System	11
1.7.3 Recovery Electronics	12
1.8 Radio Telemetry and Tracking	13
1.8.1 Ground Station	13
1.8.2 Commercial GPS Tracker	14
2 Discussion of the Roll Control Mechanism	14
2.1 Control Logic	15
2.1.1 Pre-Flight	15
2.1.2 Launch Readiness	16
2.1.3 Boost	16
2.1.4 Ascent	17
2.1.5 Descent, Landing, and Recovery	18
2.2 Controls, Modeling, and Simulation	18
2.3 Bench Test Results	18
3 Rocket Operation Assessment	19
3.1 Launch and Boost Phase Analysis	20
3.2 Coast Analysis	20
3.3 Recovery System and Descent Phase Analysis	21
4 Test Launch Actual vs. Predicted Performance	21
4.1 Peak Altitude Comparison to Expectations	22
4.2 Peak Velocity and Peak Acceleration Comparison to Expectations	23
4.3 Recovery System Performance Comparison to Expectations	23
5 Findings and Future Work	24
6 Budget	25
6.1 Booster	25
6.2 Payload	26

6.3 Miscellaneous	26
-----------------------------	----

1 Recap of Rocket Design

The ACROBAT (Angular Conservation Roll Oriented Body with Active Transmission) fuselage consists of an ogive nosecone, a body tube for the purpose of housing the electronics related to the flight instrumentation as well as the payload operation, a payload can for housing the active roll control system, a booster tube containing the parachute as well as the motor and its inner phenolic tube housing, a set of three fins, and a tail cone for holding the motor tube and phenolic tube in place. The active roll orientation system is a machined flywheel connected to a DC motor equipped with a gearbox and mounted to a machined bracket affixed to the electronics can. ACROBAT is 60.25 in (1.53 m) in length with a launch mass of 219 oz (6.21 kg)

Table 1: Test Flight Characteristics

Mass	Motor	Apogee	Max. Velocity	Max. Acceleration	Time to Apogee
13.7 lb	Cesaroni J760	4509 ft	711 ft/s	xxx ft/s ²	17.1 s

1.1 Fuselage Specifics and Dimensioning

The ogive nose cone is made of carbon fiber and has a length of 15.7 in (40 cm), a base diameter of 4.01 in (10.2 cm), and a wall thickness of 0.04 in (0.102 cm). The electronics body tube is made of wrapped carbon fiber and has a length of 10 in (25.4 cm), an outer diameter of 4.01 (10.2 cm,) and a wall thickness of 0.056 in (0.142 cm). The electronics/payload can is made of machined 6061-T6 aluminum and has a total length of 8.5 in (21.6 cm) (including the exposed and coupler portions). The coupler possesses an outer diameter of 3.9 in (9.91 cm) and a wall thickness of 0.062 in (0.159 cm). The exposed section of the can has a length of 2 in (5.08 cm), an outer diameter of 4.01 in (10.2 cm), and a wall thickness of 0.065 in (0.165 cm). The booster tube is also constructed of wrapped carbon fiber and has a length of 30 in (76.2 cm), an outer diameter of 4.01 in (10.2 cm), and a wall thickness of 0.056 in (0.142 cm). The trapezoidal fin set consists of three custom fiberglass fins, each possessing a root chord of 12 in (30.5 cm), a tip chord of 3.5 in (8.89 cm), a height of 3.5 in (8.89 cm), a sweep length of 6.6 in (16.7 cm), and a sweep angle of 62°. The tail cone is made of 6061-T6 machined aluminum with a length of 2.5 in (6.32 cm) and an initial diameter of 4.01 in (10.2 cm). Two nylon 1010 rail buttons, one at the center of mass and the other centered between the fins at the base will be used. They will be mounted opposite the camera.

1.2 Internal Components of Booster Section

As previously mentioned, the rocket motor casing will be housed in a phenolic tube. The phenolic tube is affixed to centering rings made of 1/8th inch Finnish Birch aircraft plywood. The fins have notches on their bases which interlock with the centering rings. The centering rings, phenolic tube, and fins are all bonded with 635 Thin epoxy resin from U.S. Composites, Inc.

1.3 Diagram of Rocket

Figure 1 is a visual cutaway of ACROBAT, with specific attention drawn to the centers of pressure and gravity of the rocket. The center of gravity of the rocket lies 33.696 in (85.6 cm) from the tip of the nose cone, and the center of pressure of the rocket lies 38.926 in (98.9 cm) from the tip of the nose cone.

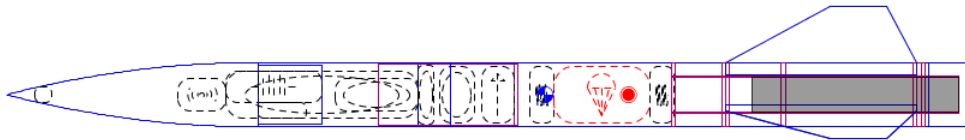


Figure 1: Diagram of the rocket with CG and CP.

1.4 Construction Techniques

A 48" section of carbon fiber tube was purchased from Public Missiles with three fin slots pre-cut. The two carbon fiber body tubes used in the rocket were cut to length with a miter saw. The coupler sections on the aluminum payload and ejection can were cut to the inner diameter of the carbon fiber body tubes using a lathe. G10 fins and plywood centering rings and bulkhead were cut using a CNC mill. Holes used to secure the sections of the rocket together were cut with a drill press. The mounting plates for the flywheel and ejection electronics were machined by the UNL Machine Shop.

The centering rings were affixed to the phenolic motor tube using the 4:1 635 Thin Epoxy system with a cure time of two hours. After the resin had fully cured, the phenolic tube was inserted into the booster section of the rocket. Resin was mixed with phenolic microballoons to increase its viscosity. The resin was then used to affix the centering rings to the booster section by applying resin to the centering rings through the fin slots. Two small notches were made in each of the fin slots so resin could be added to the booster internals after the fins had been inserted. After curing, each fin was resined into place by applying thickened resin to the internal edge of the fin and then internally filleting the fins with more resin. Fins were aligned using a laser-cut fin template to ensure each fin was perpendicular to the booster tube and spaced 120° apart from each other. After the fins

had been fully resined into place, the notches in the fin slots were filled with JB Weld and then the fins were filleted with thickened resin.



Figure 2: External fin fillets directly after resin application.

The electronics sled was 3D printed using a MakerBot Z18 printer. PLA plastic with 15% infill was used with an extruder temperature of 215°C.



Figure 3: ACROBAT fully disassembled showing all internals.



Figure 4: ACROBAT fully assembled at the test launch site.

1.5 Stability Analysis

Flight performance was analyzed for four scenarios: no wind, mild wind (2 m/s), medium wind (4.47 m/s), and high wind (8.94 m/s). Wind came from due East for each simulation. The high wind scenario corresponds to the maximum wind speed allowed by NAR rules. Wind turbulence was taken at 10% for each scenario (i.e. the wind speed standard deviation was 10% of the average wind speed). OpenRocket was used for flight simulations. The International Standard Atmosphere (ISA) was used for determinations of flight performance. The rocket has a static stability of 1.3 calibers. The center of pressure lies at 38.9 in (98.9 cm) from the tip of the nose cone, with the center of gravity at 33.696 in (86.1 cm). Minimum stability occurs immediately after launch rod clearance, and is predicted to not fall below 1 caliber for all wind conditions simulated. Stability is shown to drop below 1 caliber immediately before apogee, however, this does not represent a concern as this is due to the shifting of the center pressure as the rocket begins to turn as it reaches apogee. Maximum stability occurs immediately after motor burnout and is predicted to attain approximately 1.8 calibers for all wind conditions. See Figure 20 on page 24 for plots of stability versus time for each wind condition. The stability condition is expected to be fulfilled for all points during the flight.

1.6 AV-Bay Design

1.6.1 Hardware

The active roll control system utilized by the rocket is composed of a flywheel machined of AISI 1020 steel affixed to a VexPro VersaPlanetary 3:1 Gearbox and its accompanying VersaPlanetary Integrated Encoder. The gearbox and flywheel are driven by a VexPro BAG motor. The entire assembly is attached to a mounting plate made of 6061 T6 aluminum attached to the fuselage. The flywheel is attached to a 0.5 inch (1.27 cm) gearbox hex shaft by two VexPro heavy duty shaft collars, one above and one below. Components were designed to be lightweight yet strong enough to handle high power rocketry dynamics. The flywheel consists of a central hub and a thin-walled cylinder connected by 6 spokes. The mounting plate is a short disk with a raised outer edge. This outer edge has four threaded holes for mounting to the aluminum payload can. The plate also has four holes for the gearbox screws and a central hole for the shaft.

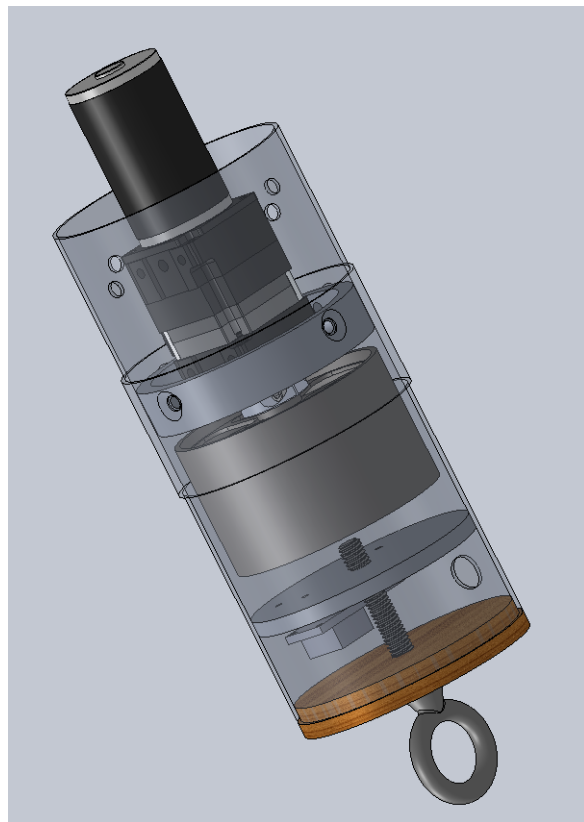


Figure 5: SolidWorks Rendering of Payload Can with Roll Control System

1.6.2 Flight Avionics

The flight avionics package performs several functions critical to the roll control mechanism and radio telemetry. The flight package is driven by a Teensy 3.6 Microcontroller Unit (MCU), which is powered by a 180 MHz ARM Cortex-M4 microcontroller. This is a powerful 32-bit microcontroller with support for a variety of hardware and software protocols. The Teensy also includes an onboard MicroSD card reader, MicroUSB connector, and support for up to 6 VDC external power. The Teensy platform is Arduino compatible, using a programmer plugin called Teensyduino. This allows easy modification and configuration of Arduino libraries for use with this microcontroller board. It will be powered by a 3.7 VDC lithium-polymer battery.

The Inertial Measurement Units outlined in the PDR have been replaced with a single Adafruit BNO055 Absolute Orientation Sensor. This sensor has been chosen instead of the two MPU-9250 arrangement because of its high rate of data collection, simplicity in programming logic, form factor, and due to its ability to output absolute pitch, roll, and yaw, simplifying data collection and programming for determining the rocket's heading during flight. The data collected from this new sensor will be used to determine the output to the motor controller.

Due to the implementation of the CAN bus in VexPro hardware, it is impossible to use precise control techniques with the Talon SRX motor controller without using VexPro logic units. Instead, a RoboClaw Solo 60A motor controller has been selected. This controller can be operated in a variety of control modes over a simple RS-232 serial interface, which is natively supported by the Teensy MCU with no additional software libraries. This motor controller has a similar size and shape to the Talon controller, and is powered by the same 3 Cell Lithium-Polymer battery described previously.

A standalone Wing HD camera will be used to record the flight and view the orientation LEDs, which will be mounted in front of the camera. Two LEDs will be used to denote the roll procedure, with each light indicating a roll direction, and both lights being used to indicate either "orientation hold" or system standby. A BMP180 barometer is also included for recording altitude, temperature, and pressure data to further improve the flight model. These sensors are powered via a common 3.3V line output by the Teensy.

Other changes in the design of the rocket since the preliminary design report center around the design of the electronics bay layout. The initial design did not consider the nose cone coupler, meaning components did not have enough clearance to fit properly. The battery was moved to a more central position and the camera was moved further down toward the DC motor to increase the ease of assembly and allow the nose cone to fit properly.

1.7 Constructed For Safe Flight and Landing

1.7.1 Structural Analysis

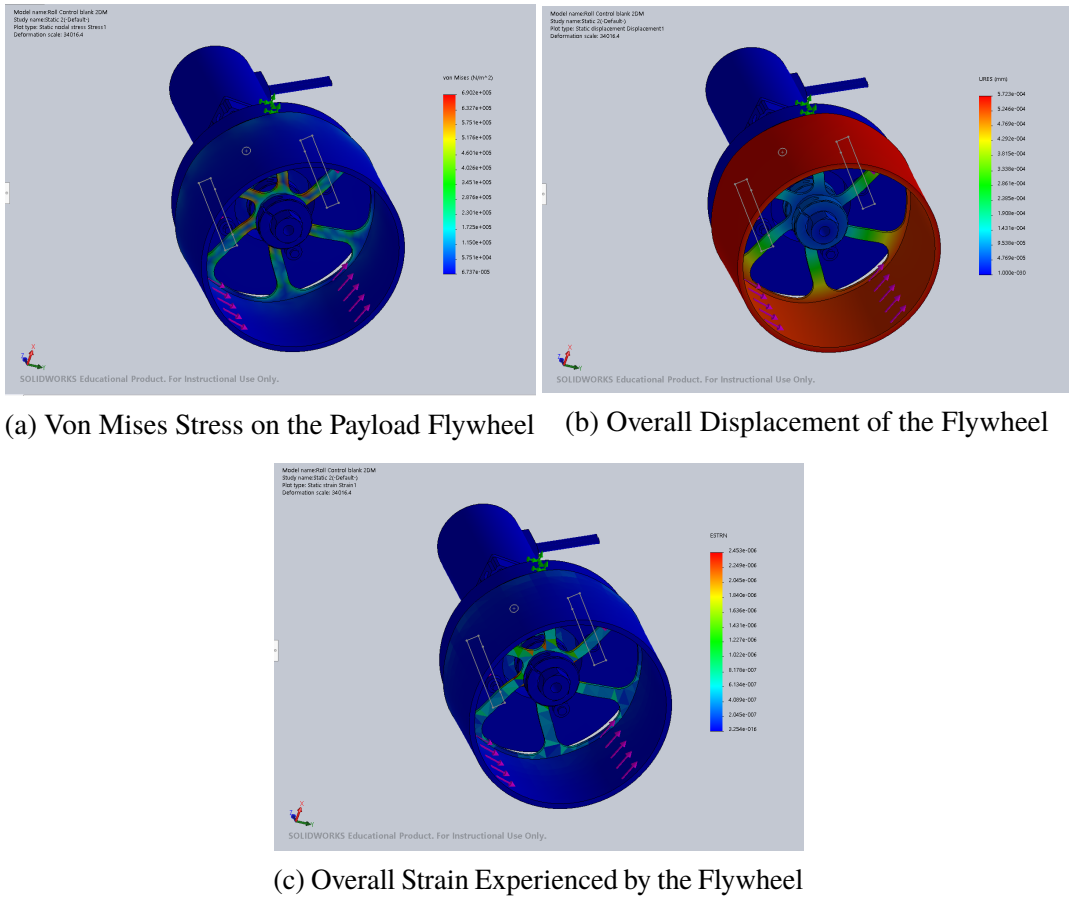
Finite Element Analysis (FEA) was done using the built-in simulation feature of SolidWorks. This was especially important for the flywheel, which will be potentially spinning over one thousand rpm and will be experiencing potentially extreme amounts of torque. Of particular concern was the ability of the spokes to handle the torque as a result of the flywheel's high rate of rotation. FEA was therefore conducted as a static study of torque on the system.

To create an accurate simulation of the potential effects of torque on the system, a reasonable value for torque experienced by the flywheel needed to be determined. This was done by determining the moment of inertia of the flywheel itself and making an estimate for the acceleration of the flywheel based on the BAG motor specifications. Using values of $2.12 \text{ lb}\cdot\text{in}^2$ for the moment of inertia and 104.7198 rad/s^2 , the estimated torque on the flywheel is approximately $0.065 \text{ N}\cdot\text{m}$, which is below the value of $0.4 \text{ N}\cdot\text{m}$, the stall torque of the BAG motor. This indicated that the motor would still be able to run with the flywheel attached without interference.

Figure 6a showcases the extent to which von Mises stress (an indicator at which a ductile material will yield) acts on the flywheel. The maximum amount of stress acting on the flywheel at any point is 690.2 kPa, which is significantly less than 410 MPa, the minimum yield strength of AISI 1020 hot-rolled steel. This showcases that the material in this orientation and shape is strong enough to withstand the stresses acting upon it during flight operations.

Figure 6b and Figure 6c are visual representations of the resultant displacement and strain, respectively, due to the application of torque on the flywheel. As can be noted from the figures, the amount of deformation experienced by the flywheel is negligible and its stiffness essentially counteracts the strain it experiences. The data gathered from this study was instrumental in the final design of the flywheel and helped to ensure that it would be a stable, strong design.

Figure 6: FEA of the Flywheel for Von Mises Stress, Overall Displacement, and Overall Strain



During ascent, the flywheel is programmed to not become active until 2 seconds after motor burnout. This is done not only to meet competition requirements but to prevent any instability caused by rotation during motor burn. Additionally, the flywheel is programmed to stop rotation before apogee so any rotation of the rocket will not cause parachute deployment issues or tangling of the shock cord.

1.7.2 Recovery System

A single deployment parachute system was used to recover the rocket. This parachute is deployed at apogee by electronically controlled ejection charges as well as a redundant time-based motor ejection charge.

To safely recover the rocket at a descent rate of less than 24 ft/sec (7.3 m/s), a Fruity Chutes Iris Ultra Compact 60 inch parachute was selected, having a drag coefficient of 2.2. This parachute is housed in the forward end of the booster section which allows the motor ejection charge to be fully operational. It is attached to the rocket by 8 ft (1.53 m) of 1/4 in. (6.35mm) flat nylon shock cord.

The shock cord is epoxied to the booster on the phenolic tube and is also attached to the payload can of the rocket with an eyebolt. The parachute is deployed at apogee using main and backup black powder ejection charges facing downward. Both the eyebolt and the charges are mounted on a plywood bulkhead at the aft end of the payload can. In addition to the plywood bulkhead, there is an additional aluminum bulkhead separating the flywheel and ejection electronics that is welded to the payload can. The eyebolt is threaded onto this bulkhead.

1.7.3 Recovery Electronics

The recovery electronics consist of a StratoLogger SL100 Altimeter, a two-cell lithium polymer battery, a key switch, and an e-match. The altimeter, battery, and key switch are housed in the payload can in the space between the aluminum and plywood bulkheads. The key switch is mounted on the inside edge of the payload can and is accessible from the outside when the rocket is completely assembled. Leads from the ejection terminals of the altimeter run to a terminal block on the other side of the wooden bulkhead. The e-matches are attached to the terminal block instead of running through the bulkhead directly to the altimeter. This allows for faster and easier launch preparation. 1 inch (2.54 cm) copper pipe caps hold the black powder ejection charges. Two grams (0.07 oz) of black powder was experimentally determined as the minimum amount to achieve separation of at least 3 feet.



Figure 7: Frame of video captured for ejection charge testing.



Figure 8: Rocket separation after the 2 grams of black powder ejection charge test.

A Jolly Logic Chute Release is used to open the parachute at a predetermined altitude in windy conditions to prevent excessive drift.

1.8 Radio Telemetry and Tracking

To complete the bonus communication challenge, the flight avionics package includes a 2.4 GHz XBee Pro radio communications module. This transmitter will be used to receive commands from the ground station before flight, and to telemeter data during the flight. The telemetry data will include roll orientation data, velocity and position, altitude, and the status of the roll control system. During the descent, the system will report useful information about the flight for quick analysis, including maximum altitude, velocity, and other interesting flight data.

The Teensy is responsible for sending and receiving data from the XBee and performing the appropriate actions. The XBee is connected to the Teensy via simple serial communication and will operate at the highest Serial data rate that provides error-free, high-speed data telemetry. The XBee is powered by the common 3.3 VDC line.

1.8.1 Ground Station

The ground station consists of an Arduino Uno R3, an SD Card shield, an XBee Pro 2.4Ghz RF Module, and a laptop. This will allow ground control to program the rocket commands prior to flight and collect and display telemetry data in real time for in-flight analysis. Data received through

telemetry will be logged to the SD card for submission.

1.8.2 Commercial GPS Tracker

A BRB900 GPS TX/RX tracking device will be included in the nose cone of the rocket, in addition to the radio telemetry system. This is to satisfy competition requirements and to provide confirmation of data received from flight telemetry.

2 Discussion of the Roll Control Mechanism

The roll control mechanism designed for this competition is a reaction wheel mechanism. A reaction wheel is a flywheel used for attitude control of a rocket, satellite, or other air or space craft. When the rotation rate of the flywheel is changed, the craft begins to counter-rotate relative to the flywheel, due to conservation of angular momentum. This allows for precise rotations of the craft without changing the aerodynamic properties of the craft, such as is the case with aerodynamic control surfaces, or requiring the use of additional propellant in a reaction control system (RCS).

The program for the roll control monitoring system is written using the Arduino IDE, and includes native Arduino and Teensy libraries, libraries from hardware manufacturers, and modifications of existing libraries made by industry professionals and enthusiasts.

Prior to flight, orientation commands are collected from the Xbee based radio telemetry system. This user input is used to populate tables that will be read to determine the heading that the rocket should hold or roll towards. Pre-flight procedures and commands are similar for each of the two competition flights in order to minimize the necessity for reprogramming the system in the field.

The roll control mechanism relies on orientation data from the BNO055 sensor to determine the current heading of the rocket, in order to calculate the motor parameters for the reaction wheel. The Teensy 3.6 performs data collection and calculation using the Arduino PID Controller library to output the correct motor speed and direction. These values are fed to the Roboclaw motor controller, which provides power to the motor in accordance with this control scheme.

Throughout the flight, linear and angular velocity, altitude, orientation, motor speed, and other measurables are recorded and logged to an onboard SD card. Orientation and other data critical to the operation of the roll control mechanism are telemetered to the ground throughout the flight at a rate of 10Hz. This data is logged from motor ignition to just before touchdown, to build a complete picture of the rocket's flight performance and the function of the roll control mechanism.

2.1 Control Logic

The programming logic of the reaction wheel can be broken down into several regimes, which are shown in the figure below.

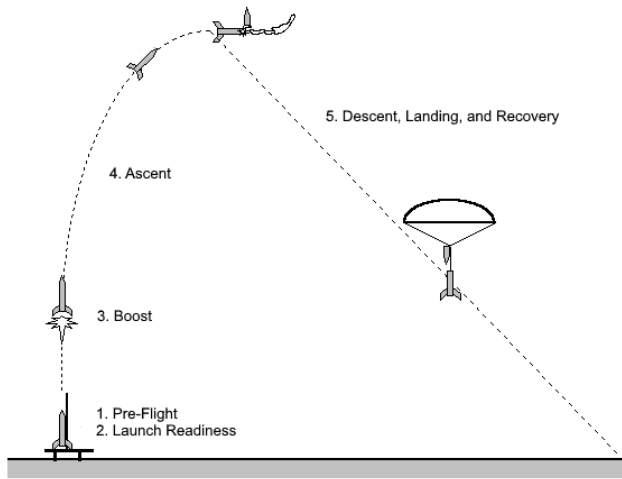


Figure 9: Diagram of Flight Program Regimes

2.1.1 Pre-Flight

During the Pre-Flight procedures, power to the MCU and Motor Controller is turned on and initial calibration steps are done by the MCU to initialize sensors and hardware. A brief radio transmission is sent to the ground station to verify the status of sensors and to confirm that radio telemetry is operational.

The IMU is calibrated according to the manufacturer's specifications. This includes holding the avionics bay stationary to calibrate the gyroscope, moving in various directions to calibrate the magnetometer, and rotating the system around an axis to calibrate the accelerometer. When this is completed, the system waits for flight programming from the radio telemetry system.

Depending on which flight is being programmed, the program will request different information in order to program the flight. For the first flight, no additional information is required. The default heading to hold is due south, and this is hard-coded into the program. For the second flight, which requires orienting the rocket to several different headings will require some user input. This input includes the number of headings per “cycle”, which is the number of headings before the series repeats, each individual heading, the rotation direction required to get to that heading, and the time to hold each heading. These values are populated into several arrays that are read in order to move to each heading.

After the programming is complete, the system will enter a standby state, awaiting an additional

radio input to tell the rocket to arm the launch detection system, entering the launch readiness phase.

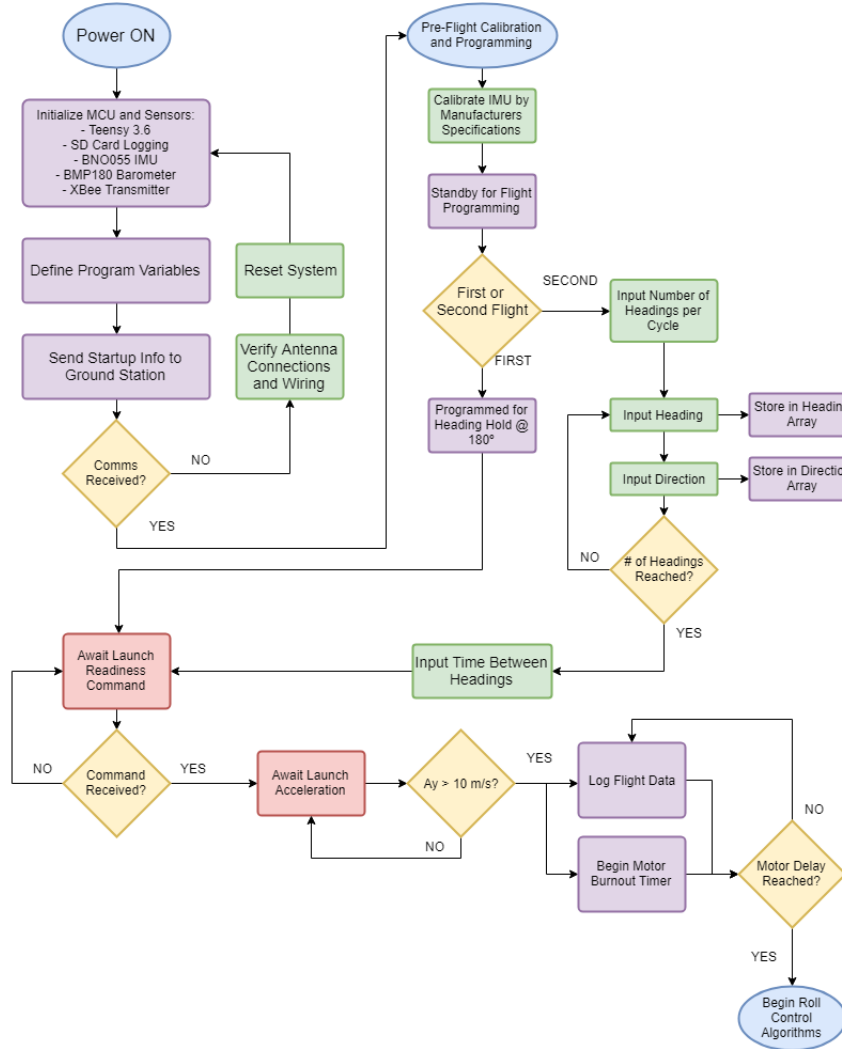


Figure 10: Pre-Flight to Motor Burnout Flowchart.

2.1.2 Launch Readiness

In this phase of the program, the rocket is awaiting launch detection. In order to detect launch, the program polls the accelerometer, awaiting a sudden increase in vertical acceleration (i.e. $A_y > 10 \text{ m/s}^2$). When this acceleration is detected, a “Launch detected” message is sent and data logging and telemetry begins.

2.1.3 Boost

During motor burn, data logging and telemetry continues for a predetermined time delay, which accounts for the motor burn time and the required delay after motor burn.

2.1.4 Ascent

After the delay is completed the roll control algorithms will take over and attempt to orient the rocket to follow the programmed instructions. Both flights rely on just two roll control functions: a Heading Hold function, and a Rocket Roll function.

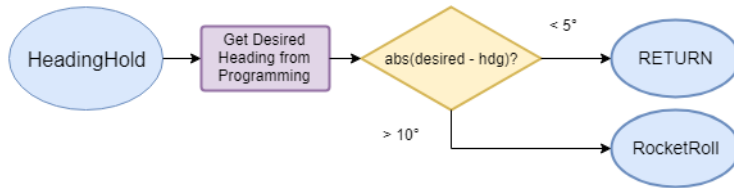


Figure 11: Heading Hold Logic Flowchart

The Heading Hold function commands the rocket to hold a specific heading for a preset period of time. In the first flight, this time is until apogee is reached. The current heading is read from the IMU and the difference from the expected heading is calculated. If the difference between the two is greater than 10°, the function will call the Rocket Roll function to roll the rocket back towards the nominal heading, in the correct direction. This will ideally correct for any slight changes in heading due to aerodynamic forces keeping the rocket within 10° of the expected heading.

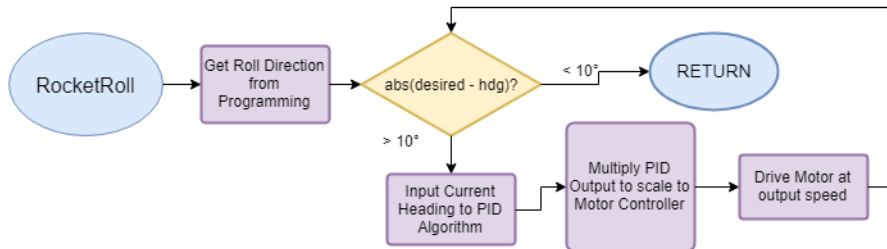


Figure 12: Rocket Roll Logic Flowchart

Rocket Roll is the primary function in which the rocket orientation changes. This function is used to rotate the rocket to a new heading in a certain direction. Using the heading and direction programmed before flight, the program will use the current direction to calculate the motor speed. The motor speed is defined by a Proportional-Integral algorithm, which was derived and fine-tuned using a Simulink model (see Controls, Modeling, and Simulation). The speed will change as the angle between the current and desired heading decreases, allowing for a responsive, yet accurate orientation change. When the angle is less than 10 degrees, the algorithm will be completed, to allow for small misalignment in the IMU sensor measurement.

In the second flight, the program will alternate between Heading Hold, and Rocket Roll as necessary, in order to follow the correct sequence of events defined in the competition instructions.

2.1.5 Descent, Landing, and Recovery

At apogee, the motor will be stopped, in order to allow safe recovery of the rocket, and to comply with competition requirements. Additional data will be logged during descent to completely log the rocket's flight path. Data collection will end when the rocket senses that it has landed. All flight data will be logged, and the system will enter a standby state awaiting recovery.

2.2 Controls, Modeling, and Simulation

In order to determine how the reaction wheel would affect the rocket orientation, a mathematical model was developed and recreated in Simulink that would accurately and reliably simulate the flywheel performance. This model was used to determine initial values for the PID Control parameters input to the Arduino PID library.

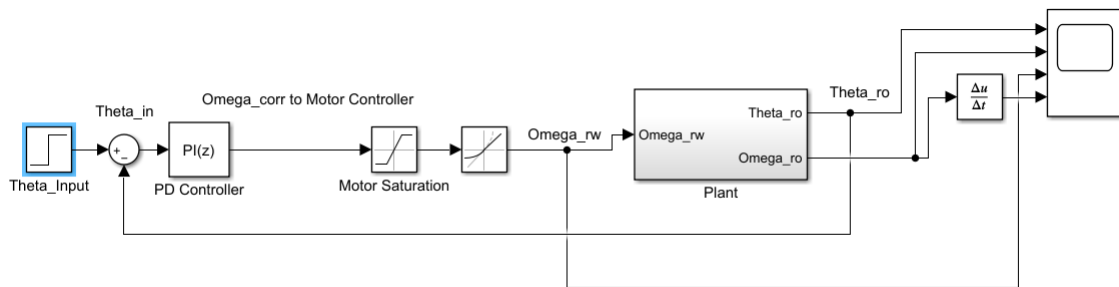


Figure 13: Simulink Model used to Model Flywheel Performance

The PID Controller combines the current heading and a control algorithm to determine how the rocket will be affected by a change in flywheel velocity. This model was implemented in the program using the native Arduino PID library. Fine-tuning the model suggested that a 180 degree rotation would be completed in under 2 seconds, and bench test results confirmed this estimate.

2.3 Bench Test Results

In order to test the performance of the roll control mechanism, a test stand was built using a bearing and two pieces of particle board. The test platform was built so that mass could be added to the platform to simulate the moment of inertia of the rocket. The roll control mechanism can be securely mounted to the center of the rotating board, to best simulate the rocket rolling.



Figure 14: Reaction Wheel Test Platform.

Due to time constraints, the bulk of the testing performed using the test platform has been to verify programming logic and the accuracy of sensor data. Additional testing was performed to fine-tune the PID controller parameters, to improve the responsiveness and accuracy of the mechanism.

3 Rocket Operation Assessment



Figure 15: ACROBAT on the launch rod at test flight.

3.1 Launch and Boost Phase Analysis

Slow motion footage of the rocket showed it took 35 frames to clear the launch rod. At a frame rate of 240 frames per second, this translates to clearance of the 8 foot launch rod in 0.15 seconds. During the boost phase, the maximum velocity of 711 feet per second (217 m/s, $M = 0.63$) occurred directly after motor burnout at 2.05 seconds at an altitude of 505 feet (154 m) AGL.

3.2 Coast Analysis

The rocket coasted for 15.05 seconds following motor burnout. The total ascent phase of the rocket lasted for 17.1 seconds from launch to apogee. For the test launch, the roll control unit was inactive, so its in-flight performance cannot be analyzed. This was due to an error in mounting the accelerometer. The flight program was written to detect launch by sensing a positive acceleration. The accelerometer was mounted upside-down, and so a positive acceleration was not sensed. The roll control unit sensed a positive acceleration at apogee, and began to function during the descent. From the onboard camera, a natural coasting roll rate between 0.53 and 0.63 Hz in the counter-clockwise direction was recorded. This was assessed by using a small pond near the launch pad as a reference point and counting frames between appearance of the pond at the left edge of the window. A maximum apogee of 4509 feet (1374 m) AGL was recorded by the Stratologger.



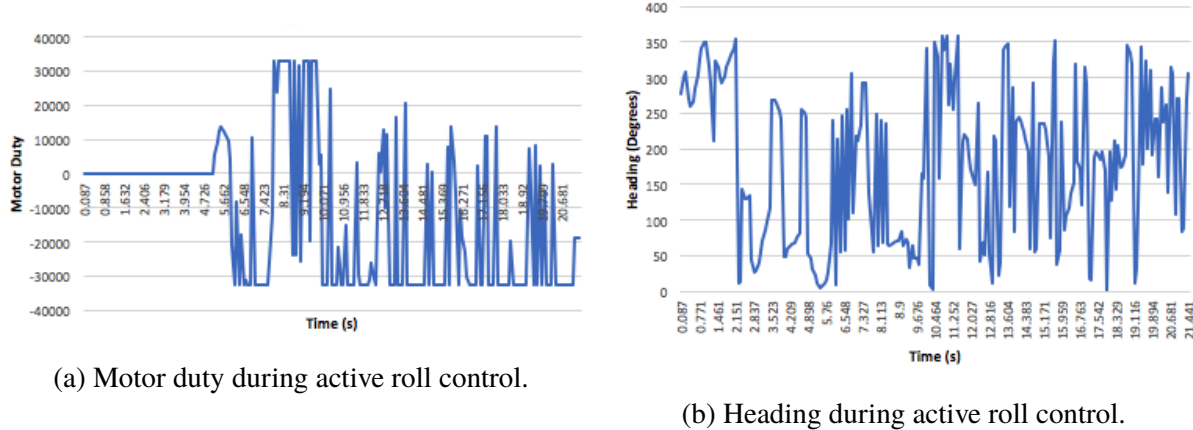
Figure 16: Pond as viewed from the internal camera onboard ACROBAT.

3.3 Recovery System and Descent Phase Analysis

The parachute was deployed by the electronic ejection charge using 2 grams of black powder. The motor ejection charge delay was set to 16 seconds after burnout. From the flight audio, it is evident that the electronic ejection is what caused separation, as only one deployment event can be heard. Had the electronic ejection failed, two deployment events would have been heard before separation. The Jolly Logic Chute Release was programmed to open at relatively high altitude of 1000 feet AGL was chosen. Because the parachute had not yet been tested by the team on a rocket, 1000 feet was chosen to ensure the parachute had adequate time to fully open. Altitude data indicates the parachute took approximately 100 feet to deploy after the parachute release opened.

Before the parachute opened, the rocket reached terminal velocity at 78 ft/s (24 m/s). After the parachute opened, terminal velocity and ground hit speed was 12 ft/s (3.7 m/s). As a note, these velocities are vertical velocities and do not factor in any lateral movement caused by wind. During the descent phase the roll control unit became active. Video evidence showed a rapid roll rate of the payload can. Recovery of data showed the while roll control unit was trying to keep a heading of 180°tumbling of the rocket led to erratic control behavior.

Figure 17: Motor Duty and Heading During Active Roll Control



4 Test Launch Actual vs. Predicted Performance

OpenRocket was used to simulate launches. Due to uncertainties in wind speed, the medium wind scenario served as the prediction for flight performance. This assumed an average wind speed of 10 mph (4.5 m/s) with a turbulence of 10% (standard deviation of 1 mph (0.45 m/s)).

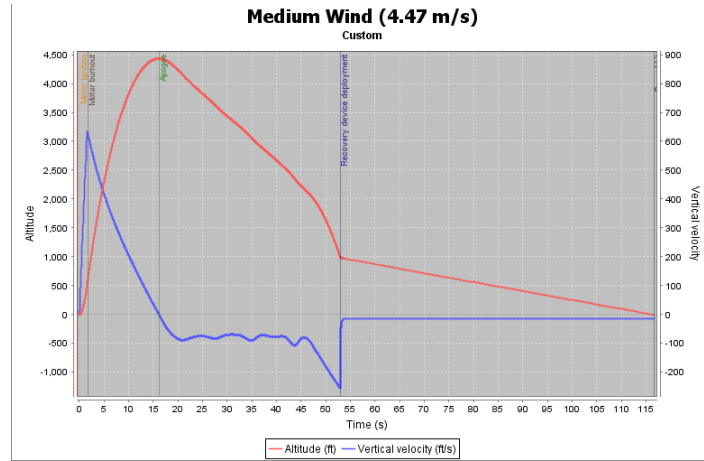


Figure 18: Full predicted flight altitude and velocity in medium wind conditions.

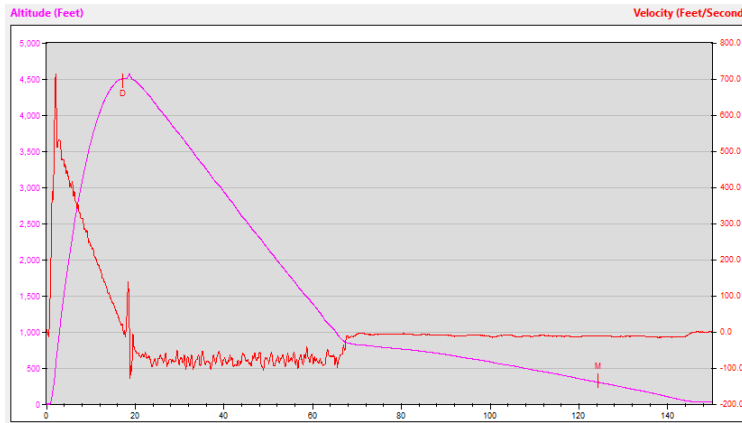


Figure 19: Actual test flight altitude and velocity as reported by the onboard Stratologger.

4.1 Peak Altitude Comparison to Expectations

The peak altitude predicted by OpenRocket was 4545 feet. The actual apogee was 4509 feet. This represents an error of 0.7%. The difference is likely due to differences in the rocket motor thrust. The reported motor burn time for the Cesaroni J760 is 1.7 seconds. From the velocity data, the burn time was closer to 2.05 seconds. The motor data used by OpenRocket only accurate to within 15%. The difference in burn time represents at 17% error in the OpenRocket thrust curve data. Additionally, environmental conditions run in OpenRocket were different than those experienced during test launch. The higher apogee is partially a result of the actual average windspeed being lower than the 10 mph used in the OpenRocket data.

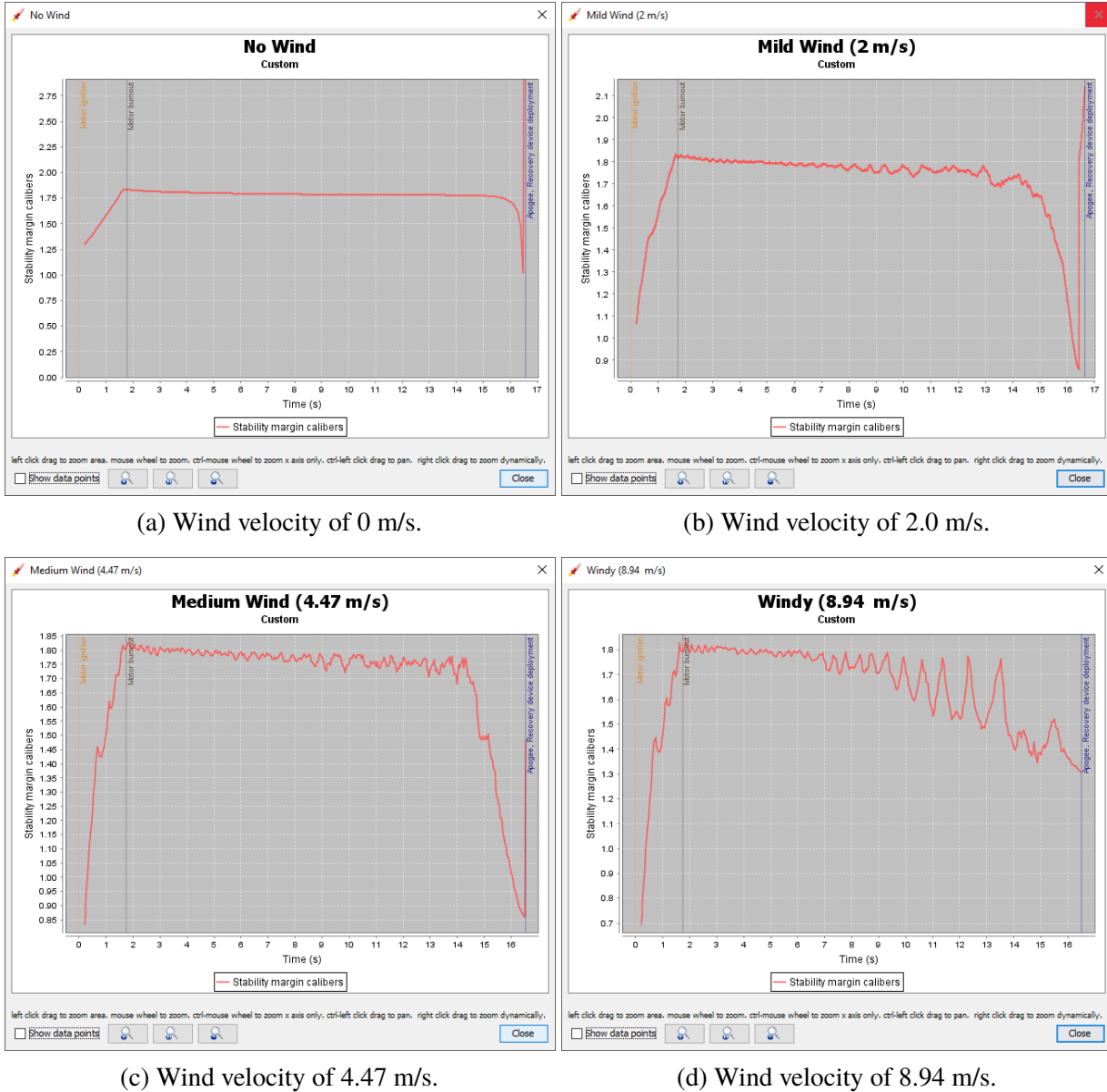
4.2 Peak Velocity and Peak Acceleration Comparison to Expectations

OpenRocket predicted a peak velocity of 624 ft/s, while the actual peak velocity was 711 ft/s. This represents an error of 12.2%. As noted before, differences in motor thrust data are likely the largest contributing factor to the error between predicted and actual velocity and acceleration. Additionally, because velocity and acceleration were not measured directly and instead integrated from altitude, it is likely that there is propagation of error from the polynomial regressions.

4.3 Recovery System Performance Comparison to Expectations

ACROBAT separated at apogee as predicted. The predicted velocity at deployment was 326 ft/s. This represents a significant error as compared to the actual deployment velocity of 78 ft/s. The error is due to OpenRocket's inaccuracy in simulating the terminal velocity of the separated rocket. Ground hit velocity was predicted to be 15.8 ft/s, or a 31% error to the actual ground hit velocity of 12 ft/s. The difference in ground hit velocity is due to differing environmental conditions. Average windspeed was slightly lower than predicted, which would account for a lower ground hit velocity. Additionally, the actual ground hit velocity may be higher than what was reported by the Stratologger, as the device does not consider lateral velocity components.

Figure 20: Simulated stabilities for all wind velocities



5 Findings and Future Work

The flight performance of ACROBAT is as expected, and no changes to external features of the rocket will be made. However, a redesign of the electronics is necessary to ensure proper launch detection. Additionally, the electronics sled will need to be redesigned to better accommodate the electronics. Inspection of the rocket after launch found the only damage was the failure of the JB Weld affixing the key switch to the side of the aluminum payload can. It is thought that the ejection charge directly above the key switch caused fracturing in the brittle epoxy. A 3D printed shim will be used in the

future to increase the surface area that can be resined to the payload can. Additionally, the phenolic microballoon-thickened 635 epoxy will be used in lieu of JB Weld due to its higher elasticity.

6 Budget

One room and one van were removed from the initial budget.

Table 2: Overall Budget

Category	Price Per Unit	Quantity	Cost
Lodging	\$400.00/night	3 nights	\$1200.00
Vehicle Rental	\$428.15/van	1	\$428.15
Gas	\$200/van	1	\$200.00
Materials	\$1858.05	n/a	\$1858.05
Registration Fee	\$400.00	n/a	\$400
Contingency fund	\$700.00	n/a	\$700
		Total	\$4786.20

6.1 Booster

The cost of the booster is \$1034.97. A itemized list can be found in Table 3.

Table 3: Booster Budget

Item	Supplier	Quantity	Cost
54mm 3-Grain Case	Apogee	1	\$69.39
Tailcone	AeroPack	1	\$54.00
Pro-54 Delay Adjustment Tool	Apogee	1	\$29.37
54mm Standard Rear Closure	Apogee	1	\$42.75
Cesaroni J760-19A White Thunder	CS Rocketry	2	\$185.90
60" Iris Ultra Parachute	Fruity Chutes	1	\$225.00
Chute Release	Jolly Logic	1	\$129.95
Eyebolt	McMaster-Carr	1	\$12.21
54mm phenolic tube	Public Missiles	1	\$14.99
Carbon Fiber Tubes	Public Missiles	1	\$239.95
Finnish Birch Aircraft Plywood	Aircraft Spruce	1	\$56.38
Natural G10 Sheet	ePlastic	1	\$71.46
		Total	\$1164.36

6.2 Payload

The cost of the payload is \$641.22. An itemized list can be found in Table 4. The major changes from the PDR are the purchase of a new IMU and motor controller.

Table 4: Payload Budget

Item	Supplier	Quantity	Cost
HD Wing Camera	Hobby King	1	\$31.19
Turnigy 5000mAh LiPo Pack	Hobby King	1	\$28.18
VersaPlanetary Integrated Encoder	VEX	1	\$49.99
BAG Motor	VEX	1	\$24.99
VersaPlanetary Gear Box	VEX	1	\$34.99
VersaPlanetary 3:1 Gear Kit	VEX	1	\$10.99
High Strength Clamping Collar	VEX	2	\$9.98
Talon SRX	VEX	1	\$89.99
Talon SRX Encoder Breakout Board	VEX	1	\$9.99
Talon SRX Data Cable	VEX	1	\$14.99
Roboclaw Solo 60A Motor Controller	Pololu	1	\$99.95
BNO055 Absolute Orientation Sensor	Adafruit	1	\$35.99
Machining Costs	UNL Machine Shop	1	\$200.00
Total			\$641.22

6.3 Miscellaneous

Other costs are \$230.02. An itemized list can be found in Table 5

Table 5: Misc. Budget

Item	Supplier	Quantity	Cost
Foam Paint Brush	Amazon	1	\$12.99
Dust Mask	Amazon	1	\$13.99
Nitrile Gloves	Amazon	1	\$10.14
Polypropylene Coverall	Amazon	1	\$45.95
635 Thin Epoxy System	US Composites	1	\$71.00
Nose Cone	Public Missiles	1	\$75.95
Total			\$230.02